Efficient Time-Domain Approach for Linear Response Functions

Michel Panhans and Frank Ortmann*
Center for Advancing Electronics Dresden, Technische Universität Dresden, 01062 Dresden, Germany
and Department of Chemistry, Technische Universität München, 85748 Garching bei München, Germany

(Received 20 January 2021; accepted 19 May 2021; published 29 June 2021)

We derive the general Kubo formula in a form that solely utilizes the time evolution of displacement operators. The derivation is based on the decomposition of the linear response function into its time-symmetric and time-antisymmetric parts. We relate this form to the well-known fluctuation-dissipation formula and discuss theoretical and numerical aspects of it. The approach is illustrated with an analytical example for magnetic resonance as well as a numerical example where we analyze the electrical conductivity tensor and the Chern insulating state of the disordered Haldane model. We introduce a highly efficient time-domain approach that describes the quantum dynamics of the resistivity of this model with an at least 1000-fold better performance in comparison to existing time-evolution schemes.

DOI: 10.1103/PhysRevLett.127.016601

Introduction.—The Kubo formalism [1] is a powerful and universal theoretical tool to connect the complex microscopic dynamics of condensed matter systems with their macroscopic thermodynamic properties. Within this framework, linear susceptibilities relate any physical observable to any other perturbing forces exerted by the experimenter and can thus explain diverse material properties such as electrical conductivity or magnetic susceptibility. Many discoveries such as the quantum Hall effects [2–5], intrinsic spin Hall effects [6,7], or quantum spin Hall effects [8–10] have been explained using linear response theory. In addition, it is used to describe magnetic resonance absorption [11], the theory of the anomalous Hall effect in the Dirac equation [12], the bulk viscosity of quark-gluon matter [13], the thermal conductivity of disordered harmonic solids [14], or linear absorption spectra in metals and semiconductors [15].

The Kubo formalism allows for large-scale numerical calculations to describe quantum systems, which elude an analytical description such as complex nanoscale systems [16–18] or when disorder or electronic correlations are present. Great efforts were therefore spent in the last two decades to work on efficient numerical implementations of Kubo formulae in the field of electronic transport [19,20]. Many numerical implementations of Kubo formulae [21–28] have been developed to optimize the description and better understand the transport physics of quantum systems and connect it to macroscopic transport phenomena and experiments. A key requirement of efficient numerical strategies is to avoid the diagonalization of the Hamiltonian matrix and elaborate on linear-scaling approaches, which is particularly challenging in the case of off-diagonal tensor components of the response function [20].

In this Letter, we present a decomposition of linear response functions into a time-symmetric and a time-antisymmetric part and find that they can solely be expressed in terms of displacement operators at equal time, which eventually enables an efficient implementation and computation. We relate this representation to the well-known form of the quantum fluctuation-dissipation theorem [29] that directly connects susceptibilities and power spectra. We find a natural generalization of the description of cross-power spectra of arbitrary pairs of perturbation forces and response observables. This enables the efficient description of transverse response phenomena such as Hall effects, spin Hall effects, or other tensor quantities (e.g., transversal magnetization effects, anisotropic diffusion-tensors, etc.) at the same footing as the longitudinal response. This unified description makes the development of specific algorithms unnecessary.

Kubo formulae.—The general Kubo formula for the linear response of observable A in the presence of a small but time-dependent perturbation $H'(t)$ of the quantum system with the Hamiltonian $\hat{H} = \hat{H}_0 + \hat{H}'(t)$ can be written as [1]

$$\mathrm{Tr}(\hat{\rho}(t)\hat{A}) = \mathrm{Tr}(\hat{\rho}_0\hat{A}) + \frac{i}{\hbar}\int_{-\infty}^{t} dt' \mathrm{Tr}(\hat{\rho}_0[\hat{H}_\mathrm{I}'(t'), \hat{A}(t)]), \quad (1)$$

with the time-dependent density operator $\hat{\rho}(t)$ that is driven by the unperturbed Hamiltonian $\hat{H}_0$ and the equilibrium density operator $\hat{\rho}_0$ (canonical or grand canonical [30]) that describes the quantum system in the absence of the perturbation. $\hat{H}_\mathrm{I}'(t') = e^{it'\hat{H}_0/\hbar}\hat{H}'(t')e^{-it'\hat{H}_0/\hbar}$ is the conventional perturbation operator in the interaction picture and $\hat{A}(t) = e^{it\hat{H}_0/\hbar}\hat{A}(0)e^{-it\hat{H}_0/\hbar}$ is the Heisenberg time evolution of $\hat{A}$.

If the perturbation is characterized by an arbitrary time-dependent modulation function $F(t)$ coupled to an operator $\hat{B}(0)$, i.e., $\hat{H}'(t) = -F(t)\hat{B}(0)$, the general Kubo formula reads

$$\mathrm{Tr}(\hat{\rho}(t)\hat{A}) = \mathrm{Tr}(\hat{\rho}_0\hat{A}) + \int_0^\infty dt' F(t-t') f_{AB}(t'), \tag{2}$$

with the response function

$$f_{AB}(t) = -\frac{i}{\hbar}\mathrm{Tr}(\hat{\rho}_0[\hat{B}(0), \hat{A}(t)]). \tag{3}$$

While a great number of examples for perturbations of this form exist, such as electric or magnetic fields, we emphasize that the following results do not assume a special form of the Hermitian operators $\hat{A}$ and $\hat{B}$. Central objects in our study are the displacement operators $\Delta\hat{A}(t)$ and $\Delta\hat{B}(t)$ that are defined as $\Delta\hat{A}(t) = \hat{A}(t) - \hat{A}(0)$ and $\Delta\hat{B}(t) = \hat{B}(t) - \hat{B}(0)$ [31]. The first result is the following theorem.

Theorem 1.—The response function $f_{AB}(t)$ can be written in the form

$$f_{AB}(t) - f_{AB}(0) = \frac{1}{2\hbar}\mathcal{D}^-_{AB}(t) + \frac{1}{2\hbar}\tan\left(\frac{\beta\hbar}{2}\frac{d}{dt}\right)\mathcal{D}^+_{AB}(t), \tag{4}$$

where we have defined the displacement operator anticommutator function (DAF)

$$\mathcal{D}^+_{AB}(t) = \mathrm{Tr}(\hat{\rho}_0\{\Delta\hat{A}(t), \Delta\hat{B}(t)\}) \tag{5}$$

and the displacement operator commutator function (DCF)

$$\mathcal{D}^-_{AB}(t) = -i\mathrm{Tr}(\hat{\rho}_0[\Delta\hat{A}(t), \Delta\hat{B}(t)]), \tag{6}$$

in which the square brackets and the curly brackets denote the commutator and the anticommutator, respectively.

One frequently encounters a special situation, namely, that the response function of interest reads $f_{\dot{A}B}(t)$, i.e., it includes an observable that is associated to a time derivative $\dot{A}$. In such cases we obtain a related theorem.

Theorem 2.—Consider that, if additionally to the assumptions of Theorem 1, the response function of interest $f_{\dot{A}B}(t)$ contains an observable defined as $\dot{\hat{A}} = (i/\hbar)[\hat{H}_0, \hat{A}]$, the linear response $\mathrm{Tr}(\hat{\rho}_0(t)\dot{\hat{A}})$ can be written as

$$\mathrm{Tr}(\hat{\rho}_0(t)\dot{\hat{A}}) = \int_0^\infty dt' F(t-t') f_{\dot{A}B}(t'), \tag{7}$$

with

$$f_{\dot{A}B}(t) = \frac{1}{2\hbar}\frac{d}{dt}\mathcal{D}^-_{AB}(t) + \frac{1}{2\hbar}\tan\left(\frac{\beta\hbar}{2}\frac{d}{dt}\right)\frac{d}{dt}\mathcal{D}^+_{AB}(t). \tag{8}$$

The proof of the theorems is provided in the Appendix [32].

Equation (4) is a specific representation of the linear response function $f_{AB}(t)$ of an arbitrary pair of observables A and B, whose connection to the conventional cross-correlation function will be shown further below. Owing to symmetry relations $\mathcal{D}^-_{AB}(t) = \mathcal{D}^-_{AB}(-t)$ and $\mathcal{D}^+_{AB}(t) = \mathcal{D}^+_{AB}(-t)$, the response function $f_{AB}(t)$ is expressed by a decomposition into a time-symmetric part $f^{\mathrm{ts}}_{AB}(t) = f_{AB}(0) + \mathcal{D}^-_{AB}(t)/2\hbar$ and a time-antisymmetric part $f^{\mathrm{ta}}_{AB}(t) = \tan(\frac{\beta\hbar}{2}\frac{d}{dt})\mathcal{D}^+_{AB}(t)/2\hbar$. We note that in the special case of $\hat{B} = \hat{A}$ the response function reads $f_{AA}(t) = \tan(\frac{\beta\hbar}{2}\frac{d}{dt})\mathcal{D}^+_{AA}(t)/2\hbar$; while if $\hat{B} = \dot{\hat{A}}$ one finds $f_{A\dot{A}}(t) = f_{A\dot{A}}(0) + \mathcal{D}^-_{A\dot{A}}(t)/2\hbar$. Their time evolution therefore depends only on either of the two functions DAF or DCF in contrast to $f_{AB}(t)$ and $f_{\dot{A}B}(t)$ where both are required. We further emphasize that these results do not exploit any time-symmetry properties of the operators or observables A and B that are sometimes used to demonstrate Onsager-Casimir relations (OCRs) [33,34], but are independently obtained and valid even in the absence of any time symmetry for the operators. Indeed the OCR connects the time reversal to the exchange of the operators ($\hat{A}$ and $\hat{B}$), a connection which will be discussed further below.

Considering the exchange of the operators in Eqs. (5) and (6), we trivially obtain $\mathcal{D}^+_{AB}(t) = \mathcal{D}^+_{BA}(t)$ and $\mathcal{D}^-_{AB}(t) = -\mathcal{D}^-_{BA}(t)$ as well as $f^{\mathrm{ta}}_{AB}(t) = f^{\mathrm{ta}}_{BA}(t)$ and $f^{\mathrm{ts}}_{AB}(t) = -f^{\mathrm{ts}}_{BA}(t)$. Again this is different to the OCRs since in the latter case a symmetry of the Hamiltonian needs to be assumed (e.g., the magnetic field needs to be reversed), which is not the case in the above relations. The absence of this assumption allows us to derive this more general approach.

Furthermore, $\mathcal{D}^+_{AB}(t)$ and $\mathcal{D}^-_{AB}(t)$ satisfy the Cauchy-Schwarz inequality $|\mathcal{D}^{+(-)}_{AB}(t)| \leq \sqrt{\mathcal{D}^+_{AA}(t)\mathcal{D}^+_{BB}(t)}$ as a strict upper limit for arbitrary $\hat{A}$ and $\hat{B}$. In the special case when $\hat{B} = \hat{A}$ the equality for $\mathcal{D}^+_{AA}(t)$ holds. However, for $\hat{B} = \dot{\hat{A}}$ the DCF satisfies the uncertainty relation $|\mathcal{D}^-_{A\dot{A}}(t)| \leq \sqrt{\mathcal{D}^+_{AA}(t)\mathcal{D}^+_{\dot{A}\dot{A}}(t)}$.

Connection to the cross-correlation function and its time symmetry.—The quantum version of the cross-correlation function $\mathcal{S}_{AB}(t)$ is defined by the symmetrized cross-correlation function [29]:

$$\mathcal{S}_{AB}(t) = \frac{1}{2}\mathrm{Tr}(\hat{\rho}_0\{\hat{B}(0), \hat{A}(t)\}), \tag{9}$$

which is a real valued function in accordance with the classical correlation function $\mathcal{S}^{\mathrm{class}}_{AB}(t) = \langle\rho_0 B(0)A(t)\rangle$ in

which $B(0)$ and $A(t)$ always commute. We now show that the decomposition of $\mathcal{S}_{AB}(t)$ into its time-symmetric and time-antisymmetric parts results in a representation with displacement operators $\Delta\hat{A}(t)$ and $\Delta\hat{B}(t)$.

Theorem 3.—Using the definitions of the DAF and the DCF, the decomposition of $\mathcal{S}_{AB}(t)$ into its time-symmetric and time-antisymmetric parts reads

$$\mathcal{S}^{\mathrm{ts}}_{AB}(t) = \mathcal{S}_{AB}(0) - \frac{1}{4}\mathcal{D}^{+}_{AB}(t), \tag{10}$$

$$\tan\left(\frac{\beta\hbar}{2}\frac{d}{dt}\right)\mathcal{S}^{\mathrm{ta}}_{AB}(t) = -\frac{\hbar}{2}f_{AB}(0) - \frac{1}{4}\mathcal{D}^{-}_{AB}(t). \tag{11}$$

The proof of Eqs. (10) and (11) is provided in the Appendix [32]. The displacement-operator form for the response function in Eq. (4) and for the correlation function according to Eqs. (10) and (11) results in

$$f_{AB}(t) = -\frac{2}{\hbar}\tan\left(\frac{\beta\hbar}{2}\frac{d}{dt}\right)\mathcal{S}_{AB}(t), \tag{12}$$

which is the fluctuation-dissipation theorem expressed in the time domain since it relates the response function $f_{AB}(t)$ with the cross-correlation function $\mathcal{S}_{AB}(t)$.

Numerical aspects of possible implementations.—Equation (4) shows that the response function is, apart from its initial value $f_{AB}(0)$, solely determined by the simultaneous displacements that are expressed by $\Delta\hat{A}(t)$ and $\Delta\hat{B}(t)$ and not by the operators $\hat{A}(t)$ and $\hat{B}(t)$ themselves. This form has two advantages: it can be exploited efficiently in numerical approaches and it avoids possibly ill-defined quantities such as diverging expectation values. An important example for the latter is the dipole operator in periodic systems [35]. In Fig. 1 we illustrate this aspect by analogy to geometric vectors and represent the action of the operators $\hat{A}(t)$, $\hat{A}(0)$, and $\Delta\hat{A}(t)$ on an arbitrary state $|\psi\rangle$ in the Hilbert space as such vectors (with their norms $N_{\hat{A}(t)} = \|\hat{A}(t)|\psi\rangle\|$, etc.). Instead of

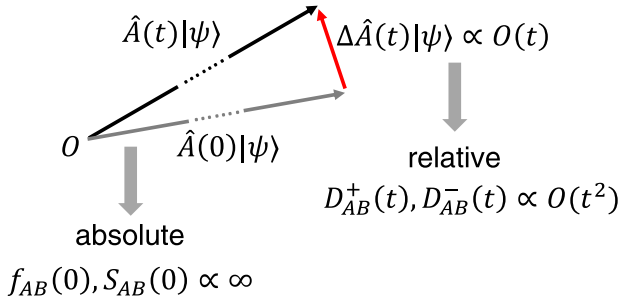

FIG. 1. Geometric interpretation of the time evolution of the change of the response function $f_{AB}(t) - f_{AB}(0)$. Only the small displacement vectors after operator action with $\Delta\hat{A}(t)$ [and $\Delta\hat{B}(t)$ equivalently] need to be calculated instead of the large vectors related to the operators $\hat{A}(t)$ or $\hat{A}(0)$.

dealing with the "large vectors," i.e., large numbers for $N_{\hat{A}(t)}$ and $N_{\hat{A}(0)}$, it is sufficient to use the "small vector displacements" (with small norm $N_{\Delta\hat{A}(t)}$) and avoid the calculation of quantities that are potentially extremely large (or infinite), which is always unpractical in the quantitative analysis of any macroscopic system. More precisely, we see that the DAF and the DCF are numerically well conditioned, because they evolve as $\mathcal{O}(t^2)$ at the starting point $t = 0$, in contrast to correlation functions that involve $\hat{A}(t)$ directly. Thus, we conclude that the evolution of the response function $f_{AB}(t)$ away from its reference $f_{AB}(0)$ can be expressed by only the simultaneous displacement operators of the observables A and B, suggesting an accurate iterative time-propagation approach.

Another aspect is of equal importance because Eq. (4) or Eq. (8) allows for a *simultaneous* simulation of both diagonal and off-diagonal tensor components for arbitrary linear responses. This time-domain approach represents a generalization over present charge-transport approaches [20]. In particular for the electrical conductivity, the time-domain approach derived in this Letter complements the Kubo-Bastin formula in the energy domain, which has been successfully used to study electron transport in topological systems and twisted bilayer graphene [28,36].

At the same time, the simulation of diagonal and off-diagonal matrix elements on equal footing in the same algorithm allows minimizing discrepancies due to different numerical approaches. This is particularly relevant when combining matrix elements such as for the calculation of the resistivity from diagonal and off-diagonal conductivities.

Series expansion of the displacement functions.—We now provide some useful relations involving the displacement functions $\mathcal{D}^{+}_{AB}(t)$ and $\mathcal{D}^{-}_{AB}(t)$ that let us find the coefficients of their Taylor series expansion around $t = 0$. First, we find an important equivalence between the displacement functions $\mathcal{D}^{+}_{AB}(t)$, $\mathcal{D}^{-}_{AB}(t)$, $\mathcal{D}^{+}_{\dot{A}\dot{B}}(t)$, and $\mathcal{D}^{-}_{\dot{A}\dot{B}}(t)$, namely,

$$\frac{d^2}{dt^2}\mathcal{D}^{+}_{AB}(t) = 4\mathcal{S}_{\dot{A}\dot{B}}(0) - \mathcal{D}^{+}_{\dot{A}\dot{B}}(t), \tag{13}$$

$$\frac{d^2}{dt^2}\mathcal{D}^{-}_{AB}(t) = -2\hbar f_{\dot{A}\dot{B}}(0) - \mathcal{D}^{-}_{\dot{A}\dot{B}}(t). \tag{14}$$

Since $\mathcal{D}^{+}_{AB}(t)$ and $\mathcal{D}^{-}_{AB}(t)$ are both time symmetric, their Taylor series expansion contains only even powers of t. As a consequence, Eqs. (13) and (14) provide a recurrence relation for their expansion coefficients. Because $\mathcal{D}^{+}_{AB}(t)$, $\mathcal{D}^{-}_{AB}(t)$ and also all higher order displacement functions, e.g., $\mathcal{D}^{+}_{\ddot{A}\ddot{B}}(t)$ and $\mathcal{D}^{-}_{\ddot{A}\ddot{B}}(t)$ vanish at $t = 0$, we have

$$\frac{d^{2k}}{dt^{2k}}\mathcal{D}^{+}_{AB}(t)|_{t=0} = 4(-1)^{k-1}\mathcal{S}_{A^{(k)}B^{(k)}}(0), \tag{15}$$

$$\frac{d^{2k}}{dt^{2k}}\mathcal{D}^{-}_{AB}(t)|_{t=0} = 2\hbar(-1)^k f_{A^{(k)}B^{(k)}}(0), \tag{16}$$

where $A^{(k)}$ denotes the k-fold nested commutator of $\hat{H}_0$ with $\hat{A}$, i.e., $A^{(k)} = (i/\hbar)^k[\hat{H}_0, \hat{A}]_k$. Thus, the series expansion of the DAF and the DCF can be written as

$$\begin{aligned}\mathcal{D}^{+}_{AB}(t) &= 4\sum_{k=1}^{\infty}\frac{(-1)^{k-1}t^{2k}}{(2k)!}\mathcal{S}_{A^{(k)}B^{(k)}}(0)\\ &= -4\sum_{k=1}^{\infty}\frac{t^{2k}}{(2k)!}\mathcal{S}_{AB^{(2k)}}(0),\end{aligned} \tag{17}$$

$$\begin{aligned}\mathcal{D}^{-}_{AB}(t) &= 2\hbar\sum_{k=1}^{\infty}\frac{(-1)^{k}t^{2k}}{(2k)!}f_{A^{(k)}B^{(k)}}(0)\\ &= 2\hbar\sum_{k=1}^{\infty}\frac{t^{2k}}{(2k)!}f_{AB^{(2k)}}(0).\end{aligned} \tag{18}$$

We show two versions for each of these intriguing expansions to highlight that different coefficients can be used to express $\mathcal{D}^{+(-)}_{AB}(t)$. They can be calculated using both the k-fold nested commutators of $\hat{A}$ with $\hat{H}_0$ and $\hat{B}$ with $\hat{H}_0$ or, alternatively, only the $2k$-fold nested commutators of $\hat{B}$ with $\hat{H}_0$ (or $2k$-fold nested commutators of $\hat{A}$ with $\hat{H}_0$). This great flexibility allows us to choose the easiest way of calculation of such commutators.

Analytical example: Magnetic resonance of an isolated electron spin.—As a minimal-model illustration of Theorem 1 that demonstrates how the displacement functions $\mathcal{D}^{+}_{AB}(t)$ and $\mathcal{D}^{-}_{AB}(t)$ determine the linear response, we use the spin precession under a perturbative magnetic field. The unperturbed system Hamiltonian of a single electron spin with mass m_e in the presence of a large magnetic field B_z is described by $\hat{H}_0 = \hat{\sigma}_z\mu_B B_z$ with the Bohr magneton $\mu_B = \hbar e/2m_e$. Here no spin-relaxation processes due to spin-spin interaction or spin-orbit interaction are considered. The system is perturbed by an adiabatically switched oscillating and linearly polarized magnetic field $\hat{H}'(t) = -\hat{\sigma}_x\mu_B B_x F(t)$ with $B_x \ll B_z$. Its response in terms of the macroscopic expectation value of the spin vector $\mathbf{S}$ with the components $S_\alpha = \mathrm{Tr}(\hat{\rho}\hbar\hat{\sigma}_\alpha/2)$ is monitored.

Within this very simple model, we can analyze analytically the individual contributions to the response function $f_{AB}(t)$ according to Eqs. (17) and (18). With $\hat{A} = \hbar\hat{\sigma}_\alpha/2$ and $\hat{B} = \hat{\sigma}_x\mu_B B_x$ we find

$$f_{AB}(0) = \mu_B B_x \mathrm{Tr}(\hat{\rho}_0\hat{\sigma}_z)\delta_{\alpha y}, \tag{19}$$

$$\mathcal{D}^{-}_{AB}(t) = 2\hbar\mu_B B_x \mathrm{Tr}(\hat{\rho}_0\hat{\sigma}_z)\delta_{\alpha y}[\cos(\omega_L t) - 1], \tag{20}$$

$$\mathcal{D}^{+}_{AB}(t) = 2\hbar\mu_B B_x[1 - \cos(\omega_L t)]\mathrm{Tr}(\hat{\rho}_0\hat{\sigma}_x^2)\delta_{\alpha x}, \tag{21}$$

with the Larmor frequency $\omega_L = eB_z/m_e$. The application of the operator $\tan(\frac{\beta\hbar}{2}\frac{d}{dt})$ on $\mathcal{D}^{+}_{AB}(t)$ is evaluated analytically and for a single spin we can use $\mathrm{Tr}(\hat{\rho}_0\hat{\sigma}_z) = \tanh(\beta\mu_B B_z)$ and $\mathrm{Tr}(\hat{\rho}_0\hat{\sigma}_x^2) = 1$. If the perturbation field oscillates with $F(t'-t) = \lim_{\eta\to 0^+} e^{-i\omega t-\eta t}$ then the susceptibility tensor $\chi_{\alpha\beta}(\omega) = 2\mu_B\mu_0 S_\alpha(\omega)/B_\beta V\hbar$ has the components

$$\chi_{xx}(\omega) = \frac{\mu_B^2\mu_0}{\hbar V}\tanh(\beta\mu_B B_z)\frac{2\omega_L}{\omega^2-\omega_L^2}, \tag{22}$$

$$\chi_{yx}(\omega) = -\frac{\mu_B^2\mu_0}{\hbar V}\tanh(\beta\mu_B B_z)\frac{2i\omega}{\omega^2-\omega_L^2}, \tag{23}$$

in full consistence with the textbook expression for the paramagnetic susceptibility in the theory of magnetic resonance (MR) [37]. This shows that MR is correctly described with the analytical displacement functions, while the numerical evaluation allows us to describe much more complex situations of the magnetic resonance and a broader class of spin-related phenomena in the new approach. Indeed, if the system Hamiltonian $\hat{H}_0$ becomes more complex (e.g., with additional spin-orbit interaction, i.e., $\hat{H}_0 \to \hat{H}_0 + \gamma\hat{\mathbf{L}}\cdot\hat{\mathbf{S}}$, or spin-spin interactions such as in the Heisenberg model for ferro- or anti-ferromagnetic materials, i.e., $\hat{H}_0 \to \hat{H}_0 + \gamma\sum_{\langle i,j\rangle}\hat{\mathbf{S}}_i\cdot\hat{\mathbf{S}}_j$) the displacement functions $\mathcal{D}^{+}_{AB}(t)$ and $\mathcal{D}^{-}_{AB}(t)$ can rarely be expanded analytically but Eq. (4) can be evaluated efficiently by time evolution approaches [19,20]. In this work we showcase another application field, the charge carrier transport.

Numerical example: Electrical conductivity tensor of the Haldane model.—In this application, which is of foremost interest to us, the operators $\hat{A}$ and $\hat{B}$ are identified with the electric dipole moments along different Cartesian directions $e\hat{x}_\alpha$, while the modulation function is taken to be constant $F(t'-t) = F(0)$ and proportional to the electric field strength E_β. Then the linear response of the current density $\mathrm{Tr}(\hat{\rho}(t)\hat{j}_\alpha) = \sigma^{\mathrm{dc}}_{\alpha\beta}E_\beta$ with $\hat{j}_\alpha = e\dot{\hat{x}}_\alpha/V$ is described by the dc-conductivity tensor

$$\sigma^{\mathrm{dc}}_{\alpha\beta} = \frac{e^2}{V}\lim_{t\to\infty}\left(\frac{\beta}{4}\frac{\tan(\frac{\beta\hbar}{2}\frac{d}{dt})}{(\frac{\beta\hbar}{2}\frac{d}{dt})}\frac{d}{dt}\mathcal{D}^{+}_{x_\alpha x_\beta}(t) + \frac{1}{2\hbar}\mathcal{D}^{-}_{x_\alpha x_\beta}(t)\right). \tag{24}$$

We consider the classic Haldane model for honeycomb lattices [38] as a fundamental example of a topological Chern-insulator to demonstrate the theoretical and numerical description. Its Hamiltonian is defined on the graphene lattice as

$$\hat{H}_0 = -t_1 \sum_{\langle i,j \rangle} \hat{c}_i^\dagger \hat{c}_j + t_2 \sum_{\langle\langle i,j \rangle\rangle} e^{i\phi_{ij}} \hat{c}_i^\dagger \hat{c}_j + \frac{\Delta_{AB}}{2} \sum_i (\delta_{iA} - \delta_{iB}) \hat{c}_i^\dagger \hat{c}_i + \sum_i V_i \hat{c}_i^\dagger \hat{c}_i, \quad (25)$$

with the nearest-neighbor coupling t_1 and the next-nearest-neighbor coupling t_2. The electronic on site energies can be modified by an energy splitting Δ_{AB} that breaks the AB-sublattice symmetry, which, however, is taken $\Delta_{AB} = 0$ for simplicity here. Additionally, a uniform Anderson disorder potential with $-V/2 \leq V_i \leq V/2$ is applied. The next-nearest-neighbor coupling t_2 opens an energy gap Δ_T at the Dirac point. This topological gap opens because time-reversal symmetry is broken leading to an anomalous quantum Hall effect. If the unimodular phase is set to $|\phi_{ij}| = \pi/2$ such that the total net flux inside a hexagon vanishes, the topological gap has a width of $\Delta_T = 6\sqrt{3}t_2$. In Figs. 2(a) and 2(b), we show the numerical results for the energy-resolved resistivities ρ_{xy} and ρ_{xx} for different values of Δ_T, which are obtained from the time-resolved conductivity tensor in Eq. (24) taken at $t = 20\pi/t_1$. The results inside the topological gap confirm the Hall conductivity $\sigma_{xy} = e^2/h$ and the Hall resistivity $\rho_{xy} = h/e^2$ in full consistency with the disorder-free case [38] and other implementations of the Kubo formula [28] based on the Kubo-Bastin formula for the electrical conductivity [2].

In addition to the energy dependence of electron transport, we are here able to determine the time-resolved dynamics of the conductivity and the resistivity, exemplarily shown in Figs. 2(c) and 2(d). For example, the Hall plateau in σ_{xy} and ρ_{xy} emerges at early times and, for the large topological gap of $\Delta_T = t_1$, converges after 10 periods of $\tau_T = 2\pi/\Delta_T$ with a root-mean-square deviation of 0.5% relative to the analytical value [blue line in Figs. 2(c) and 2(d)]. This formation time would correspond to around 15 fs (if we take $t_1 = 2.7$ eV as a typical value for graphene). For the small gap of $\Delta_T = 0.1t_1$, the formation process is tenfold slower and shows a stronger oscillatory behavior at early times [see red curve in Figs. 2(c) and 2(d)]. Still in both cases of significant Anderson disorder ($V = 0.1t_1$), we conclude that the formation process of the topological state is stable against disorder-induced scattering. Slight differences in the convergence behavior to a plateau value are observed between the gap center and the gap edges when the strength of the Anderson disorder is comparable to the system's topological gap [see Fig. 2(b)].

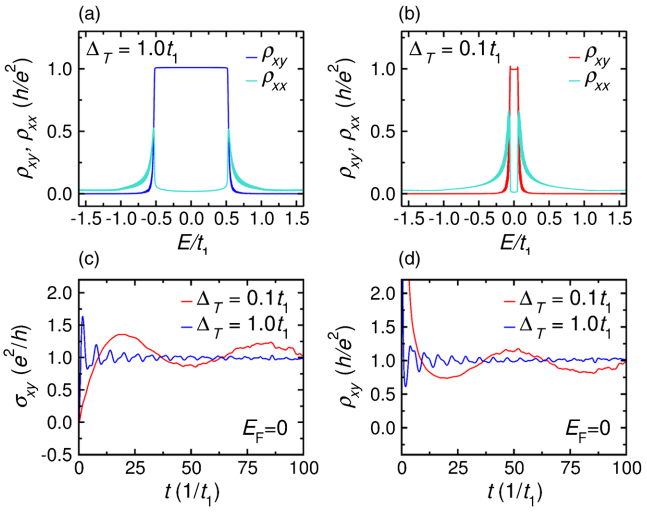

FIG. 2. (a) Longitudinal and transversal resistivity components of the Haldane model for graphene calculated from the displacement form of the Kubo conductivity. The model parameters are set to $\Delta_T = t_1$, $\Delta_{AB} = 0$ and $V = 0.1t_1$. (b) Same as in (a) but with reduced topological gap $\Delta_T = 0.1t_1$. (c) and (d): Time-resolved Hall conductivity (c) and Hall resistivity (d) at the Dirac point ($E = 0$) for both topological gap sizes.

We further emphasize that the transverse response is obtained at a very small fraction of the conventional simulation time because only $\mathcal{D}^+_{x_\alpha x_\beta}(t)$ and $\mathcal{D}^-_{x_\alpha x_\beta}(t)$ need to be propagated numerically. As compared to other linear-scaling time-domain approaches [27,39] that require a propagation of around 1000–5000 Lanczos vectors, the new time-domain approach demands the propagation of only 2–4 Lanczos vectors, which hence results in a speed-up and savings in computational time by 3 orders of magnitude.

Finally, the correspondence of the new formalism based on the expressions (4) and (8) to known forms of the Kubo formula for the electrical conductivity [1,40] is compiled in the Appendix [32] for the interested reader. There, we also discuss further limiting cases, namely, the high-temperature and the classical limit of Eqs. (4) and (8).

Conclusions.—In this work, we have derived analytic forms of linear response functions by decomposition into time-symmetric and time-antisymmetric contributions. This enables an efficient implementation and computation of transverse linear response phenomena at the same footing as the longitudinal response. Different limiting cases that are known have been reproduced. This unified description makes the development of specific algorithms unnecessary and at the same time allows us to study these responses in the time domain. As compared to other linear-scaling time-domain approaches to transverse responses, it benefits from a speed-up factor of 1000 or more. This allows the precise determination of topological effects in a time-domain approach that has not been established before.

We would like to thank the Deutsche Forschungsgemeinschaft for financial support (Projects No. OR 349/1 and OR 349/3). Grants for computer time from the Zentrum für Informationsdienste und Hochleistungsrechnen of TU Dresden (ZIH) and the Leibniz Supercomputing Centre in Garching (SuperMUC-NG) are gratefully acknowledged.

*Corresponding author.
frank.ortmann@tum.de

[1] R. Kubo, J. Phys. Soc. Jpn. **12**, 570 (1957).
[2] A. Bastin, C. Lewiner, O. Betbeder-matibet, and P. Nozieres, J. Phys. Chem. Solids **32**, 1811 (1971).
[3] P. Streda, J. Phys. C **15**, L717 (1982).
[4] H. Aoki and T. Ando, Solid State Commun. **38**, 1079 (1981).
[5] R. Yu, W. Zhang, H.-J. Zhang, S.-C. Zhang, X. Dai, and Z. Fang, Science **329**, 61 (2010).
[6] S. Murakami, N. Nagaosa, and S.-C. Zhang, Phys. Rev. Lett. **93**, 156804 (2004).
[7] J. Sinova, D. Culcer, Q. Niu, N. A. Sinitsyn, T. Jungwirth, and A. H. MacDonald, Phys. Rev. Lett. **92**, 126603 (2004).
[8] C. L. Kane and E. J. Mele, Phys. Rev. Lett. **95**, 226801 (2005).
[9] X.-L. Qi, Y.-S. Wu, and S.-C. Zhang, Phys. Rev. B **74**, 085308 (2006).
[10] B. A. Bernevig, T. L. Hughes, and S.-C. Zhang, Science **314**, 1757 (2006).
[11] R. Kubo and K. Tomita, J. Phys. Soc. Jpn. **9**, 888 (1954).
[12] A. Crépieux and P. Bruno, Phys. Rev. B **64**, 014416 (2001).
[13] F. Karsch, D. Kharzeev, and K. Tuchin, Phys. Lett. B **663**, 217 (2008).
[14] H. Sevinçli, S. Roche, G. Cuniberti, M. Brandbyge, R. Gutierrez, and L. M. Sandonas, J. Phys. Condens. Matter **31**, 273003 (2019).
[15] F. Bechstedt, *Many-Body Approach to Electronic Excitations* (Springer, Berlin, 2016).
[16] D. Van Tuan, J. Kotakoski, T. Louvet, F. Ortmann, J. C. Meyer, and S. Roche, Nano Lett. **13**, 1730 (2013).
[17] T. Markussen, R. Rurali, M. Brandbyge, and A.-P. Jauho, Phys. Rev. B **74**, 245313 (2006).
[18] S. Latil, S. Roche, and J.-C. Charlier, Nano Lett. **5**, 2216 (2005).
[19] A. Weiße, G. Wellein, A. Alvermann, and H. Fehske, Rev. Mod. Phys. **78**, 275 (2006).
[20] Z. Fan, J. H. Garcia, A. W. Cummings, J. E. Barrios-Vargas, M. Panhans, A. Harju, F. Ortmann, and S. Roche, Phys. Rep. **903**, 1 (2021).
[21] S. Roche and D. Mayou, Phys. Rev. Lett. **79**, 2518 (1997).
[22] S. Ciuchi, S. Fratini, and D. Mayou, Phys. Rev. B **83**, 081202(R) (2011).
[23] H. Ishii, N. Kobayashi, and K. Hirose, Phys. Rev. B **83**, 233403 (2011).
[24] K. Landsteiner, E. Megías, and F. Pena-Benitez, Phys. Rev. Lett. **107**, 021601 (2011).
[25] S. Plumari, A. Puglisi, F. Scardina, and V. Greco, Phys. Rev. C **86**, 054902 (2012).
[26] H. Ishii, H. Tamura, M. Tsukada, N. Kobayashi, and K. Hirose, Phys. Rev. B **90**, 155458 (2014).
[27] F. Ortmann, N. Leconte, and S. Roche, Phys. Rev. B **91**, 165117 (2015).
[28] J. H. García, L. Covaci, and T. G. Rappoport, Phys. Rev. Lett. **114**, 116602 (2015).
[29] R. Kubo, Rep. Prog. Phys. **29**, 255 (1966).
[30] For the canonical ensemble, we use $\hat{\rho}_0 = e^{-\beta\hat{H}}/\mathrm{Tr}(e^{-\beta\hat{H}})$ and for the grand-canonical ensemble we use $\hat{\rho}_0 = e^{-\beta(\hat{H}-\mu\hat{N})}/\mathrm{Tr}(e^{-\beta(\hat{H}-\mu\hat{N})})$.
[31] The term displacement operator appears in different contexts in physics with different meanings. For clarity, with displacement operator, we mean the difference of two operators: one is the Heisenberg-evolved operator and the other is its non-time-evolved operator. The general use of this term here is not restricted to any specific operator.
[32] See Supplemental Material at http://link.aps.org/supplemental/10.1103/PhysRevLett.127.016601 where we rigorously derive Theorems 1 to 3. We briefly introduce the high-temperature and the classical limit of the response functions given in Eqs. (4) and (8). Furthermore, we relate Eq. (24) to known limits of the Kubo formula for electrical conductivity.
[33] L. Onsager, Phys. Rev. **37**, 405 (1931).
[34] H. B. G. Casimir, Rev. Mod. Phys. **17**, 343 (1945).
[35] R. M. Martin, Phys. Rev. B **9**, 1998 (1974).
[36] M. Anđjelković, L. Covaci, and F. M. Peeters, Phys. Rev. Mater. **2**, 034004 (2018).
[37] N. Pottier, *Nonequilibrium Statistical Physics: Linear Irreversible Processes* (Oxford University Press, Oxford, 2009).
[38] F. D. M. Haldane, Phys. Rev. Lett. **61**, 2015 (1988).
[39] F. Ortmann and S. Roche, Phys. Rev. Lett. **110**, 086602 (2013).
[40] S. Nakajima, Prog. Theor. Phys. **20**, 948 (1958).